PII: S0032-3861(97)00030-X

Polymer Vol. 38 No. 20, pp. 5079–5084, 1997
© 1997 Elsevier Science Ltd
Printed in Great Britain. All rights reserved
0032-3861/97/$17.00+0.00

Melting behaviour, crystal transformation and morphology of sulfonated poly(ethylene terephthalate) fibres

You-Lo Hsieh* and Xiao-Ping Hu
Fiber and Polymers, Division of Textiles, University of California, Davis, CA 95616, USA
(Received 14 August 1996; revised 20 November 1996)

High temperature wide-angle X-ray diffraction (HTWAXD) has elucidated the differences in the structural changes in undrawn and crimped sulfonated poly(ethylene terephthalate) (SPET) fibres during heating from 230°C through melting. Both the heat-induced crystals and the drawing-induced crystals in the undrawn and crimped SPET fibres are triclinic. The HTWAXD data suggest that different morphologies are responsible for the distinct melting behaviour between the undrawn and drawn SPET fibres. It is thought that spherulites and bundled crystals are induced by heating and drawing in the undrawn and drawn SPET fibres, respectively. Upon heating, the undrawn fibres crystallize into spherulitic crystals ($T_m = 257$°C) whose structure do not change at temperatures approaching melting. The drawing-induced bundle crystals in the crimped fibres melt at a lower melting temperature of 249°C. The bundled crystals are oriented to the fibre axis, but highly stressed, less perfect, and smaller in size, therefore melt at lower temperatures. With increasing temperatures, the partially melted paracrystalline structure transforms into a pseudohexagonal crystalline structure before reorganizing into spherulites which melt subsequently. © 1997 Elsevier Science Ltd.

(Keywords: sulfonated poly(ethylene terephthalate) (SPET); high temperature wide-angle X-ray diffraction; melting behaviour)

INTRODUCTION

Crystallization and melting behaviour of poly(ethylene terephthalate) (PET) have been extensively studied because a wide range of crystallinity could be achieved on PET. Thermal analysis, either differential thermal analysis (d.t.a.) or differential scanning calorimetry (d.s.c.), has been by far the most common technique for such investigation[1–15]. Melting of PET with only one known crystal form has been reported to give double melting endothermic peaks[3,4,8–11]. The double endotherms have been attributed to different types of crystalline morphology (extended- or folded-chain crystals)[3], distribution of crystallite sizes and crystal perfection[2], and melt–recrystallization processes[5–9]. Earlier work attributed the lower temperature peak to the melting of the partially extended chain crystals and the higher temperature peak to the folded chain crystals[3]. Later reports have suggested the correspondence of the lower temperature endotherm to melting of the crystals grown at crystallization conditions or pre-existed in the samples[2]. The higher temperature peak is thought to be derived from melting of the recrystallized structure from heating during thermal analysis. The dependence of the lower melting temperature on the sample thermal history and experimental conditions has generally been ascribed to changes in crystallite sizes, crystallite perfection and surface structure. During heating, the partial melting and rapid recrystallization of the low-melting crystals was believed to produce more ordered, high-melting crystals[2].

A single endothermic peak has also been reported on PET crystallized at high crystallization temperatures[5], or melted at high scanning rate in differential thermal analysis[2]. The single melting endotherm is a result of merging of the melting doublet. At higher crystallization temperatures or shorter crystallization time, the higher melting endothermic peak remain at a constant temperature but diminish and eventually disappear while the lower melting endothermic peak enlarged progressively and shifted to higher temperature[2,7]. It is well recognized now that results of thermal analysis not only reflect the polymer structure originated from the processing, but also the structural transformation which takes place during heating or scanning.

Thermal analytical techniques in combination with X-ray techniques have shown to be powerful tools for melting behaviour and morphological studies of PET[5,7]. While thermal analysis profiles structural changes in PET during heating, wide angle X-ray studies of PET have focused primarily on the unit cell, crystallinity, and morphology at room temperature. Little is known about the crystalline structure and morphology in the PET fibres at elevated temperatures. One of the questions on the double melting peak concerns with structural transformation near the melting temperature. Although earlier work did not suggest any structural change between the two melting endotherms[1,3], others have shown strong evidence of structural change accompanying the melting and crystallization of PET[5].

* To whom correspondence should be addressed

The aim of this present work is to investigate the temperature dependent structural features near the melting temperatures of sulfonated PET fibres. High temperature wide angle X-ray diffraction (HTWAXD) enables structural characterization as a function of temperature. HTWAXD in conjunction with thermal analysis is used to elucidate the structural and morphological nature of thermal transitions and to help to explain the structural features associated with the double melting endotherms of SPET.

EXPERIMENTAL

Materials

Sulfonated poly(ethylene terephthalate) (SPET) (Dacron 64, du Pont de Numerous Co.) filaments were used in this study. The viscosity average molecular weight (M_v) of the SPET is 19 600 g mol^{-1} or an average degree of polymerization (DP) of 102. Two to three per cent of the aromatic rings in SPET polymer are sulfonated ($-SO_3N_a^+$). Thus the SPET contains 2–3 sulfonated units per molecule on average. Fibres from different fibre processing stages were included in this study. The 'undrawn' fibres were spun fibres immediately quenched by H_2O under tension after coming out of the spinnerets. The 'crimped' fibres are referred to those drawn after being heated at 90°C and crimped by passing through a heated stuffer-box at 90° to 100°C with the aid of steam. *Table 1* summarizes the physical properties of the SPET fibres and the PET homopolymer counterparts. The average diameter of the undrawn SPET fibres is 28.4 μm. The process of drawing and crimping reduced the diameter of the SPET fibres and increased the densities of SPET fibres.

High temperature wide angle X-ray diffraction (HTWAXD)

The high temperature X-ray scannings were performed on a Scintag XDS 2000 X-ray diffractometer equipped with a high-temperature chamber. The Cu$K\alpha$ radiation was generated at an accelerating potential of 45 kV and a tube current of 45 mA. The high-temperature chamber consists mainly of a cylindrical, double-walled and water-cooled stainless pot, an irradiation window and a heater. The heater is a tungsten metal strip which is clamped over one pair of electrodes. The high-temperature chamber was fully automated for heating with a ±1°C precision. The fibres were cut into a fine powder form and laid down onto the top of the heater. The X-ray scanning was performed in the 2θ range from 12° to 32°. Diffraction intensities were counted at 0.04°-steps and the scanning time of each step was 5 s. The X-ray scannings were performed at room temperature, and at varying temperatures from 230° to 270°C. For peak position calibration, a standard quartz powder was used. Scanning began after a 10 min-holding period. Subsequently, the experimental data were resolved and analysed by the multi-peak resolution method[16].

Differential thermal analysis

Differential thermal analyses (d.t.a.) of the studied fibres were performed on a Mettler TA 2000M system. All d.t.a. scans were performed in nitrogen from 30° to 320°C at varying heating rates. Al_2O_3 was used as the reference. About 3.5–4 mg of the finely cut fibres were compressed into small soft pellets at 10 000 psi. The reported values for melting temperatures were averages of duplicated d.t.a. runs.

RESULTS AND DISCUSSION

D.t.a. thermograms

The d.t.a. thermograms of the undrawn and crimped SPET fibres are shown in *Figure 1*. The undrawn SPET fibres exhibit a glass transition temperature (T_g) at 82.3°C and crystallize (T_c) at 128°C. A single melting endotherm is observed for the undrawn SPET fibres at 257°C. The crimped SPET fibres are semi-crystalline and oriented, thus do not exhibit glass transition nor crystallize. A double melting endotherm is observed on the crimped SPET fibres, with the lower peak temperature at 249°C and the higher melting temperature at 257°C, the same as that for the undrawn SPET fibres. In comparison with the undrawn PET fibres, the higher ΔH_f coupled with lower T_m and lower T_g of the undrawn SPET fibres suggest that SPET chains are more mobile, easier to crystallize, and form smaller crystallites but higher crystallinity from heating in the d.t.a. The smaller amplitude and broader peak width of the melting endotherm of the undrawn SPET fibres also indicate a higher level of crystallite defects and broader crystallite size distribution.

The lower-temperature melting peak of the crimped SPET fibres is believed to result from melting of the crystals formed by drawing. Our previous work showed that the lower-temperature melting peak is shifted to higher temperatures with increasing heating rates during

Table 1 Physical properties of the undrawn and crimped SPET and PET fibres

Fibre/process	Diameter (μm)	Density (g ml^{-1})	Refractive index $n_{\parallel}$	Refractive index $n_{\perp}$	Birefringence Δn
SPET					
undrawn	28.4	1.3572	1.587	1.572	0.015
crimped	18.0	1.3914	1.668	1.556	0.113
PET					
undrawn	19.3	1.3481	1.587	1.573	0.014

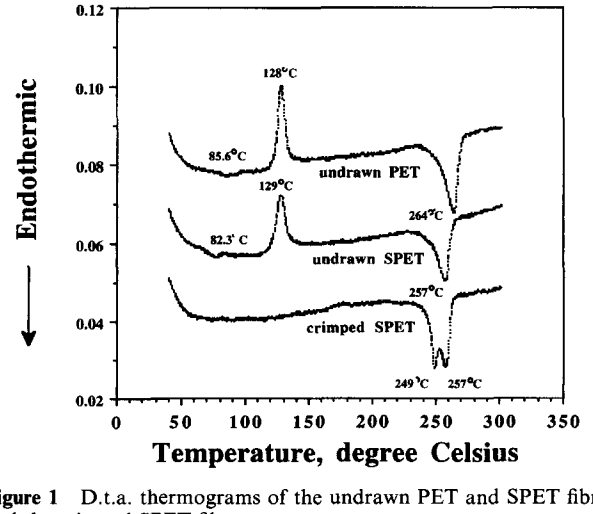

Figure 1 D.t.a. thermograms of the undrawn PET and SPET fibres, and the crimped SPET fibres

thermal analysis[2]. The increased melting temperatures are due to super heating of the drawing-induced crystals. On the other hand, the higher endothermic peak temperature of the crimped SPET fibres is similar to the T_m of the undrawn fibres at all heating rates, and is thought to be related to the melting of the heat-induced crystals during d.t.a. The effects of d.t.a.-induced crystallization decrease with increasing heating rate. At higher heating rates, the heat-induced crystallization is minimized and super heating dominates, leading to the disappearance of the T_m differences between the undrawn and the crimped fibres.

HTWAXD patterns

The wide angle X-ray diffraction (WAXD) patterns of the undrawn SPET fibres at varying temperatures are shown in *Figure 2*. At 22°C, the undrawn SPET fibres are nearly amorphous. As the temperature increases above the T_c, crystallization is induced. The WAXD pattern detected at 230°C shows that a crystalline structure has been developed. The X-ray diffraction pattern shows five peaks within the selected 2θ range and is similar to those for the isothermally crystallized PET polymers[5,8,9]. The noise level of the WAXD pattern is higher here because of the small sample size. The small sample is necessary to minimize the temperature gradient from the heater to the sample surface on which the X-ray beams were reflected.

All the diffraction traces were analysed using a previously described multiple-peak resolution method[16]. The non-crystalline region scatterings including amorphous and background scatterings were resolved using a polynomial function. A mixture of Gaussian and Cauchy functions was employed to resolve peaks in terms of peak height, peak width at half height and peak position. The WAXD pattern detected at 230°C is resolved into five peaks at 16.31°, 17.20°, 21.38°, 22.37°, 25.03°, respectively (*Figure 3*). These peak positions indicate that, upon being heated above the T_c, a triclinic crystalline structure has been induced from the undrawn SPET fibres. These peaks are assigned as $0\bar{1}1$, 010, $\bar{1}11$, $\bar{1}10$, 100 in a triclinic form, respectively. This is close to the classic crystalline structure of PET proposed by Bunn *et al.* ($a = 4.56$, $b = 5.94$, $c = 10.75$ (Å), and $\alpha = 98.5°$, $\beta = 118.0°$, $\gamma = 112.0°$)[17].

As the temperatures increases, the two-theta peak positions were reduced whereas the peak heights were increased (*Table 2*). The decreases in the 2θ angles are expected from thermal expansion. However, thermal expansion in crystals usually leads to reduced peak heights. The increased peak heights when temperature was raised from 230° to 240°C indicate that the crystallization continues as the temperature increases. Similar conclusion was made by having found the differences between the area under the crystallization peak and the area under the melting peak on the d.t.a. thermograms of several PET samples[5]. The crystallite sizes for peaks $0\bar{1}1$, $\bar{1}11$, 100 increased by 19–38% when the temperature was raised from 230 to 240°C (*Table 2*). It should be noted that the crystallite sizes calculated here are the apparent sizes which do not take crystallite defects into consideration. In fact, the defects play important roles in the X-ray line broadening. Quantitative evaluation of line broadening caused by the defects can be rather complicated. A simple approach to this is to compare the peak width at half peak height which

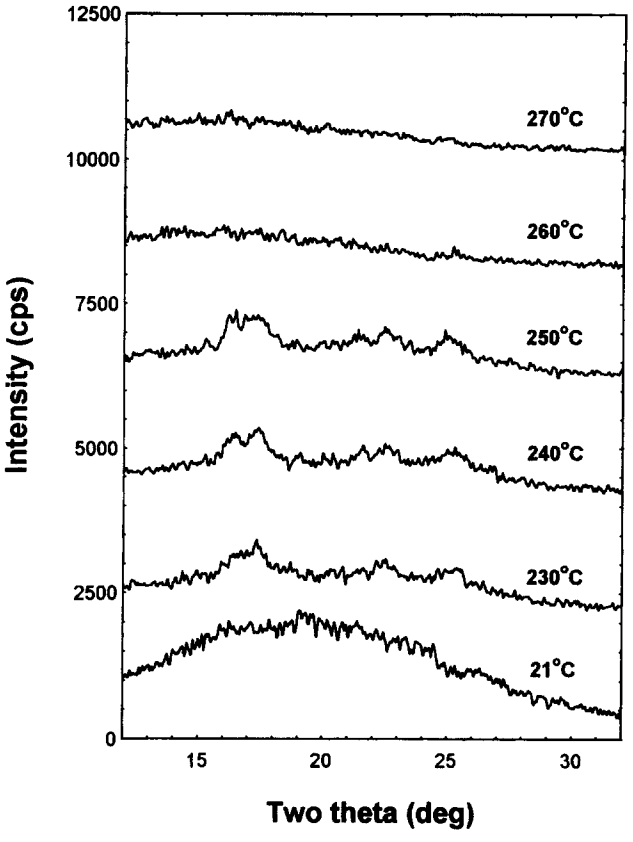

Figure 2 WAXD patterns of the undrawn SPET fibres at varying temperatures

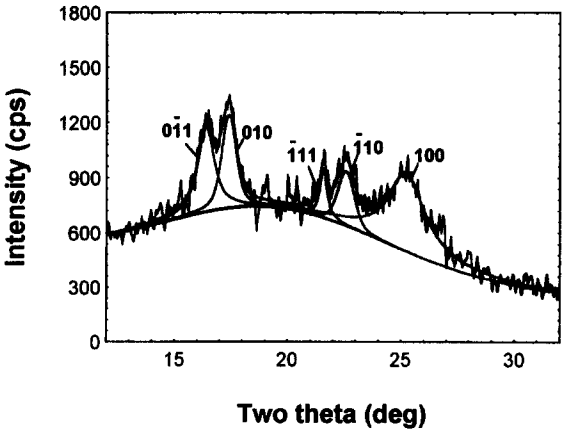

Figure 3 Resolved WAXD pattern of the undrawn SPET fibres at 230°C

reflects both the crystallite dimension and crystallite perfection. The improvement of the crystallite perfection and the increase in crystallite sizes are further confirmed by the total crystallinity increase from 15% at 230°C to 20% at 240°C. Therefore, both improvement of crystallite perfection and enlargement of crystallite sizes have been observed with temperature from 230° to 240°C.

At 250°C, the peak heights remain similar to those observed at 240°C. The crystallinity, however, was reduced from 20% at 240°C to 15% at 250°C. This reduction indicates that pre-melting has begun at about 250°C. With further temperature increases up to 260°C, all peaks diminish except the faint 100 peak (*Figure 2*). The disappearance of all the peaks at 270°C confirms that all crystals in these fibres have completely melted at this temperature.

Table 2 Resolved peak parameters, crystallinity and crystallite sizes of the undrawn SPET fibres at varying temperatures (in a triclinic crystal form)

Parameters	230°C	240°C	250°C
2θ (deg)			
$0\bar{1}1$	16.31	16.19	16.05
010	17.20	17.18	17.05
$\bar{1}11$	21.38	21.30	21.18
$\bar{1}10$	22.37	22.36	22.26
100	25.03	25.01	24.87
Height (cps)			
$0\bar{1}1$	325	463	478
010	440	507	508
$\bar{1}11$	72	263	172
$\bar{1}10$	288	304	327
100	335	411	344
Width (deg)			
$0\bar{1}1$	1.04	0.86	0.56
010	0.63	0.79	1.46
$\bar{1}11$	0.35	0.29	0.61
$\bar{1}10$	0.97	0.91	0.84
100	2.01	1.42	1.08
Crystallite size (Å)			
$0\bar{1}1$	65.7	78.1	127.0
010	94.7	88.6	56.5
$\bar{1}11$	126.8	175.0	102.9
$\bar{1}10$	75.6	78.5	76.1
100	40.1	50.4	64.9
Crystallinity (%)	15	20	15

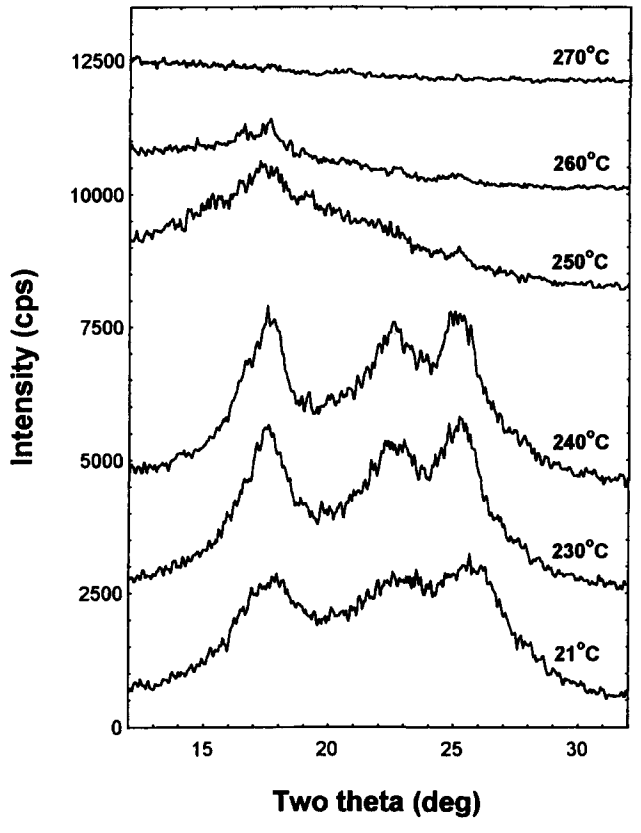

Figure 4 WAXD patterns of the crimped SPET fibres at varying temperatures

The crimped SPET fibres exhibit a crystalline structure at 22°C (*Figure 4*). The crystalline structure was induced by the drawing process and enhanced by the heat treatment during crimping. The resolved WAXD pattern shows three broad peaks and a polynomial background (*Figure 5*). These three peaks are located at 17.28°,

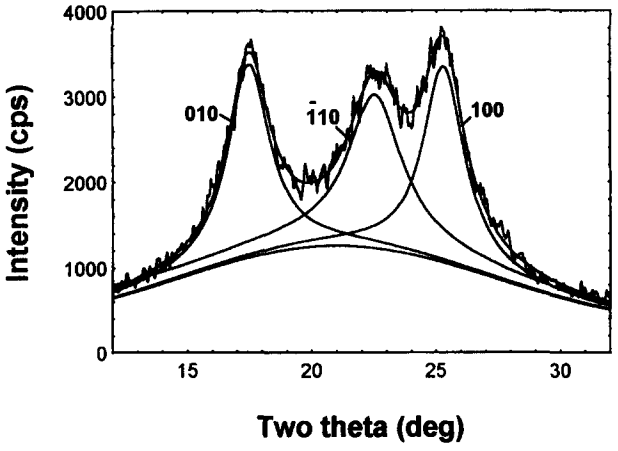

Figure 5 Resolved WAXD pattern of the crimped SPET fibres at 240°C

22.46°, and 25.69° and are very close to the two theta positions of the peaks 010, $\bar{1}10$, 100 in a triclinic form in Bunn *et al.*'s PET crystalline structure[17]. The three WAXD peaks have also been reported in literature for PET[18,19]. The absence of the peaks $0\bar{1}1$ and $\bar{1}11$ may be due to the introduction of crystallite orientation. The calculated apparent crystallite sizes for these peaks at 25°C are 31.4, 27.9 and 31.0 (Å), respectively, and the crystallinity is 58%.

As the temperature increases to 230°C, the two theta peak positions are shifted to the lower values, again due to thermal expansion. All three peak heights increase and peak widths narrow. The decreasing peak widths and increasing peaks height indicate improvement of crystallite perfection as well as crystallite dimensions. The improved perfection and the enlargement of crystallites are accompanied by a gradual decrease in crystallinity (*Table 3*). The slight decreases in peak heights at 240°C indicate beginning of melting.

With further temperature increase to 250°C, a new WAXD pattern is observed. The 010 and $\bar{1}10$ peaks disappear whereas the 100 peak is only very faintly observed. This suggests that most of the drawing-induced triclinic crystals in the crimped SPET fibres have melted. In the meantime, a new intensive peak located at 17.1° is detected. Although the intensity of this peak is not as strong as other peaks observed at lower temperatures, its appearance is definitive particularly considering the deminishing triclinic peaks. Due to melting of the triclinic crystals, it is speculated that this new peak is from the formation of a new crystalline structure. This new crystalline structure may be a pseudohexagonal form with the 100 peak at 17.1°. Therefore, solid-state structural transformation from a triclinic to a predominantly pseudohexagonal form is suggested for the crimped PET fibres between 240° and 250°C.

The WAXD pattern at 260°C shows diminishing pseudohexagonal peak 100. Two weak peaks located at 16.54° and 17.59° appear, indicating the reorganization of the melted crystals to a new crystalline structure. The new crystalline structure is similar to that generated from heating of the undrawn SPET fibres (*Figure 2*). The low (7%) crystallinity at this elevated temperature is a result of the short crystallization time. The disappearance of all the peaks at 270°C indicates that all crystals in the fibres have completely melted.

Table 3 Resolved peak parameters, crystallinity and crystallite sizes of the crimped SPET fibres at varying temperatures (in a triclinic crystal form except[a] for a pseudohexagonal form)

Parameters	21°C	230°C	240°C	250°C	260°C
2θ (deg)					
$0\bar{1}1$					16.54
010	17.28	17.24	17.21		17.59
$\bar{1}10$	22.46	22.33	22.32		
100	25.69	25.09	25.02	25.01	25.09
				17.1[a]	
Height (cps)					
$0\bar{1}1$					270
010	1588	2254	2095		478
$\bar{1}10$	1241	1709	1645		
100	1816	2289	2225	201	74
				1252[a]	
Width (deg)					
$0\bar{1}1$					0.53
010	3.04	2.00	2.12		0.58
$\bar{1}10$	3.83	2.58	2.20		
100	3.01	1.97	1.79	0.49	0.64
				4.00[a]	
Crystallite size (Å)					
$0\bar{1}1$					114.1
010	31.4	40.3	39.9		103.9
$\bar{1}10$	27.9	33.6	36.7		
100	31.0	39.7	42.3	72.8	97.3
				27.9[a]	
Crystallinity (%)	58	51	42	30	7

The d.t.a. data have shown partial melting of the drawing-induced crystals of crimped SPET at above 240°C. The effects of the 10-min holding time between X-ray scannings in HTWAXD appear to be the same as annealing. When annealed in the molten state, crystals in the crimped SPET fibres go through solid-state structural transformations from a triclinic structure to a predominantly pseudohexagonal form, and then back to a triclinic form. It is this partial melting state where both molecular mobility and residual ordered regions are present to enable the formation of new crystals which melt at a higher temperature. The residual ordered segments act as nuclei for new crystal formation. Between the drawing-induced and heat-induced triclinic crystals, there exists a predominantly pseudo-hexagonal crystal form. The pseudo-hexagonal crystals probably arise from the thermal expansion and melting of bundle-like crystals.

The HTWAXD studies of the undrawn and crimped SPET fibres show that both the heat-induced crystals and the drawing-induced crystals have the same triclinic crystalline structure. However, the differences in melting behaviour and HTWAXD patterns between the undrawn and the crimped fibres show their crystal perfection and morphology to be different. The crimped SPET fibres have higher crystallinity but smaller crystallite dimensions and poorer crystallite perfection than the undrawn counterpart. The HTWAXD data suggest that spherulites and bundled crystals are induced by heating and drawing, in undrawn and SPET fibres, respectively. This is similar to the report on high-speed spun PET fibres where spherulitic, lamellar, and fibrillar structures have been observed with increasing windup speeds[20]. The chains in the spherulites are folded whereas they are more extended in the bundled crystals. Drawing produces bundled crystals with lower crystal perfection and size whereas further heating improves either the perfection or the dimension, but not the amount, of spherulites. These different morphologies of the heat-induced and drawing-induced crystals (orientation, crystallite size and crystallite perfection) lead to different WAXD patterns.

SUMMARY

HTWAXD of the undrawn and crimped SPET fibres has shown that both the heat-induced crystals and the drawing-induced crystals in these fibres are triclinic. The crystallinity in the crimped SPET fibres are higher, but the crystals have smaller crystallite dimensions and poorer crystallite perfection than the undrawn counterpart. It is speculated that spherulites and bundled crystals are induced by heating and drawing, in undrawn and drawn SPET fibres, respectively.

The undrawn fibres crystallize with heating, but the heat-induced crystallized structure do not change upon melting. The crimped fibres, on the other hand, exhibit solid-state structural transformation from the triclinic form to the pseudohexagonal form when heated between 250° and 260°C. Further increases in temperature cause reorganization of melted crystals to a triclinic structure similar to that of the undrawn SPET fibres.

The distinct melting behaviour between the undrawn and drawn SPET fibres is attributed to their different

morphologies. The spherulites have a higher melting temperature of 257°C. The melting process continues as the temperature increases. No structural transformation is observed on the undrawn SPET fibres during heating. The drawing-induced bundle crystals have a lower melting temperature of 249°C. The bundled crystals are oriented to the fibre axis, but highly stressed, less perfect, and smaller in size, therefore melt at lower temperatures. With increasing temperatures, the partially melted paracrystalline structure transforms into a pseudo-hexagonal crystalline structure before reorganize into spherulites. The spherulitic crystals melt subsequently. These account for the undrawn SPET fibres exhibit one endothermic peak while the crimped SPET fibres show two endothermic peaks in thermal analysis.

REFERENCES

1. Roberts, R., *J. Polym. Sci.: Polym. Lett. Ed.*, 1970, **8**, 381.
2. Timm, D. A. and Hsieh, Y. L., *J. Polym. Sci.: Polym. Phys. Ed.*, 1993, **31**, 1873.
3. Bell, J. and Dumbleton, J., *J. Polym. Sci.*, 1969, **A-2**, 1033.
4. Neely, D., Davis, T. and Kibler, C., *J. Polym. Sci.*, 1970, **A-2**, 2141.
5. Holdsworth, P. and Turner-Jones, A., *Polymer*, 1971, **12**, 195.
6. Sweet, G. and Bell, J., *J. Polym. Sci.*, 1972, **A-2**, 1273.
7. Alfonso, G. C., Pedemonte, E. and Ponzetti, L., *Polymer*, 1979, **20**, 104.
8. Groeninckx, G., Reynaers, H., Berghmans, H. and Smets, G., *J. Polym. Sci.: Polym. Phys. Ed.*, 1980, **18**, 1311.
9. Groeninckx, G. and Reynaers, H., *J. Polym. Sci.: Polym. Phys. Ed.*, 1980, **18**, 1325.
10. Fontaine, F., Ledent, J., Groeninckx, G. and Reynaers, H., *J. Polym. Sci.: Polym. Phys. Ed.*, 1982, **23**, 185.
11. Gupta, V., Ramesh, C. and Gupta, A., *J. Appl. Polym. Sci.*, 1984, **29**, 3727.
12. Fatou, J. G., in *Applied Fiber Science*, Vol. 3, ed. F. Happey. Academic Press, New York, 1979.
13. Miyagi, A. and Wunderlich, B., *J. Polym. Sci.*, 1972, **A-2**, 1401.
14. Shalaby, S. W. (Chap. 3) and Jaffe, M. (Chap. 7), in *Thermal Characterization of Polymeric Materials*, ed. A. Turi. Academic Press, New York, 1981.
15. Timm, D. A. and Hsieh, Y. L., *J. Appl. Polym. Sci.*, 1994, **51**, 1291.
16. Daubeny, R. deP., Bunn, C. W. and Brown, C. J., *Proc. Roy. Soc. (Lond.)*, 1954, **A226**, 531.
17. Hindeleh, A. M., Johnson, D. J. and Montague, P. E., in *Fiber Diffraction Methods*, ed. A. D. French and K. H. Gardener, ACS Symp. No. 141. American Chemical Society, Washington DC, 1983, p. 149.
18. Goikhman, A. Sh., Pirogov, V. I., Sheiman, A. Z., Zhelevskaya, L. P., Borshch, N. A., Mal'tsevs, N. G. and Kovaleva, V. I., *Polym. Sci., USSR*, 1992, **34**, 179.
19. Murase, Y. and Nagai, A., in *Advanced Fiber Spinning Technology*, ed. T. Nakajima. Woodhead, Abingdon, 1994.
20. Diacik, I., Durcova, O., Mitterpachova, M. and Diacikova, A., *Polym. Sci. USSR*, 1990, **32**, 335.